JOURNAL OF GENERAL VIROLOGY

RESEARCH ARTICLE

López-Carrasco and Flores, *Journal of General Virology* 2017;98:1913–1922

DOI 10.1099/jgv.0.000846

The predominant circular form of avocado sunblotch viroid accumulates *in planta* as a free RNA adopting a rod-shaped secondary structure unprotected by tightly bound host proteins

Amparo López-Carrasco and Ricardo Flores*

Abstract

Avocado sunblotch viroid (ASBVd), the type member of the family *Avsunviroidae*, replicates and accumulates in chloroplasts. Whether this minimal non-protein-coding circular RNA of 246–250 nt exists *in vivo* as a free nucleic acid or closely associated with host proteins remains unknown. To tackle this issue, the secondary structures of the monomeric circular *(mc)* (+) and (−) strands of ASBVd have been examined *in silico* by searching those of minimal free energy, and *in vitro* at single-nucleotide resolution by selective 2′-hydroxyl acylation analysed by primer extension (SHAPE). Both approaches resulted in predominant rod-like secondary structures without tertiary interactions, with the *mc* (+) RNA being more compact than its (−) counterpart as revealed by non-denaturing polyacryamide gel electrophoresis. Moreover, *in vivo* SHAPE showed that the *mc* ASBVd (+) form accumulates in avocado leaves as a free RNA adopting a similar rod-shaped conformation unprotected by tightly bound host proteins. Hence, the *mc* ASBVd (+) RNA behaves *in planta* like the previously studied *mc* (+) RNA of potato spindle tuber viroid, the type member of nuclear viroids (family *Pospiviroidae*), indicating that two different viroids replicating and accumulating in distinct subcellular compartments, have converged into a common structural solution. Circularity and compact secondary structures confer to these RNAs, and probably to all viroids, the intrinsic stability needed to survive in their natural habitats. However, *in vivo* SHAPE has not revealed the (possibly transient or loose) interactions of the *mc* ASBVd (+) RNA with two host proteins observed previously by UV irradiation of infected avocado leaves.

INTRODUCTION

Within viroids, small non-protein-coding circular RNAs capable of infecting and frequently inciting disease in certain higher plants [1–7], avocado sunblotch viroid (ASBVd) [8] displays two singular features: the smallest genomic size (246–250 nt) and an A+U content (62 %) well above that of any other viroid (40–47 %) [9–11]. ASBVd, the type member of the family *Avsunviroidae*, replicates in plastids (mostly chloroplasts) through a symmetric rolling-circle mechanism [12–15]. Reiterative transcription of the infecting (+) monomeric circular *(mc)* RNA by a nuclear-encoded polymerase (NEP) translocated into chloroplasts [16] results in oligomeric head-to-tail (−) RNA intermediates, which after self-cleaving into monomeric linear *(ml)* forms via *cis*-acting hammerhead ribozymes [17] most likely acting co-transcriptionally [18], are circularized subsequently by a chloroplastic tRNA ligase [19]. The second half of the replication cycle, triggered by the *mc* (−) RNA, is the symmetric version of the first one (hence the name for this variant of the rolling-circle mechanism). Therefore, the two *mc* ASBVd (+) and (−) strands are physiologically relevant and the conformation they adopt *in vivo* are of particular interest because, lacking protein-coding ability, they should contain structural motifs crucial for different functions like replication and intra, intercellular and long-distance trafficking including invasion of reproductive tissues.

The secondary structure of the *mc* ASBVd (+) and (−) RNAs has been analysed *in silico* by searching those of minimal free energy [11, 17, 20–22]. While this thermodynamics-based methodology predicts rod-like or quasi-rod-like conformations for both strands, *in vitro* examination of the *ml* ASBVd (+) and (−) RNAs by selective 2′-hydroxyl acylation analysed by primer extension (SHAPE), complemented by gel electrophoresis and other physical approaches

Received 30 March 2017; Accepted 26 May 2017

Author affiliation: Instituto de Biología Molecular y Celular de Plantas (IBMCP), Universidad Politécnica de Valencia-Consejo Superior de Investigaciones Científicas, Valencia, Spain.

***Correspondence:** Ricardo Flores, rflores@ibmcp.upv.es

Keywords: circular RNAs; non-coding RNAs; RNA secondary structure; SHAPE *in vivo*; viroids.

Abbreviations: ASBVd, avocado sunblotch viroid; CChMVd, chrysanthemum chlorotic mottle viroid; ELVd, eggplant latent viroid; *mc*, monomeric circular; *ml*, monomeric linear; NEP, nuclear-encoded polymerase; PAGE, polyacrylamide gel electrophoresis; PLMVd, peach latent mosaic viroid; PSTVd, potato spindle tuber viroid; SHAPE, selective 2′-hydroxyl acylation analyzed by primer extension.

[23–25], has led to secondary structures exhibiting significant differences. Prominent among them is the presence [23] or absence [24] of a kissing-loop interaction stabilizing the *ml* (−) RNA.

In the present work, besides reassessing this discrepancy *in vitro* – using the *mc* (+) and (−) forms instead of their *ml* counterparts – we have applied *in vivo* SHAPE to address an intriguing conundrum: whether the predominant *mc* ASBVd (+) RNA exists *in planta* as a free nucleic acid or associated with host proteins that might provide some protection effect. Resembling the situation reported recently for the *mc* (+) form of the potato spindle tuber viroid (PSTVd) (the type member of the family *Pospiviroidae* clustering the nuclear-replicating viroids [26]), our results indicate that the *mc* ASBVd (+) form accumulates in its main subcellular habitat, the chloroplast [15, 27–29], essentially as a 'naked' RNA. This finding has significant implications for the replication and survival strategy of ASBVd and other viroids in general.

RESULTS

mc ASBVd (+) and (−) strands fold into rod- or quasi-rod-like conformations according to *in silico* predictions

Throughout the present study we have focused our attention on the *mc* ASBVd RNAs of both polarities because they are the forms that prime the two rolling-circles that operate in the symmetric replication of ASBVd. Moreover, in infected avocado, the *mc* ASBVd (+) form is by far the most abundant viroid RNA [12–14, 21], thus facilitating its analysis *in vivo* and its isolation and purification. The *mc* ASBVd (−) strand, although considerably less prevalent than its (+) counterpart, still reaches *in planta* a titre high enough to obtain the amount needed for dissection *in vitro* with several approaches. Previous thermodynamics-based predictions of the secondary structures of the *mc* ASBVd (+) and (−) RNAs, usually performed with the *Mfold* software program [30], have led to rod-like conformations that in some cases include a short bifurcation in one of the terminal domains [11, 17, 20, 21, 31]. Here we have reassessed this issue with recent versions of the same software program, and two others, considering that the high A+U content of the *mc* ASBVd (+) and (−) forms should result in secondary structures of minimal free energy less stable and more difficult to predict than those typical of other viroids.

Concerning the *mc* ASBVd (+) RNA, the three software programs, *Mfold* [30], *RNAfold* [32] and *RNAstructure* [33, 34], the first two equipped with a version for circular RNAs, produced similar rod-shaped secondary structures of minimal free energy for our variant, which differs in just one substitution (C213→U) from the reference variant (GenBank accession number J02020) [11]. However, the conformations resulting from *Mfold* and *RNAstructure* presented in the left terminal domain a short bifurcation with two hairpins, one of them replaced by a large internal asymmetric loop in the conformation generated by *RNAfold* (Fig. 1a, inset 3). In addition, *Mfold* predicted two slightly different motifs (Fig. 1a, insets 1 and 2), the first one predicted also by *RNAfold* together with another one (Fig. 1a, insets 1 and 4). The difference in free energy between the alternative conformations, however, was very low. The probability profile created by *RNAstructure* differed along the rod-like structure, being higher in the terminal domains (particularly in the left one) than in the central domain (Fig. 1a).

With regard to the *mc* ASBVd (-) RNA, the three software programs produced the same rod-like conformation, thus providing strong support for it (Fig. 1b). As with the *mc* ASBVd (+) RNA, the probability pattern created by *RNAstructure* differed along the rod-like-shaped conformation. A point worthy of note is that the three software programs predicted a more stable conformation for the *mc* ASBVd (+) RNA (ΔG° at 37 °C between −73.8 and −69.3 kcal mol^{-1}) than for the *mc* ASBVd (-) RNA (ΔG° at 37 °C between −56.9 and −50.0 kcal mol^{-1}).

mc ASBVd (+) and (−) forms adopt predominant secondary structures *in vitro* that can be discriminated by non-denaturing PAGE

We next tried to validate the *in silico* predictions and, particularly, whether the *mc* ASBVd (+) and (−) RNAs adopted a predominant conformation in solution and, in such a case, whether a physical distinction could be made between them. The *mc* ASBVd (+) form was directly isolated by denaturing PAGE from viroid-enriched RNA preparations from infected tissue; we assumed that the minor contamination with its co-migrating *mc* (−) counterpart, probably less than 10 % [13], should not interfere with the subsequent analysis. The *mc* ASBVd (−) form was prepared by circularization with a wheat germ extract of the *ml* ASBVd (−) RNA resulting from *in vitro* self-cleavage of a dimeric head-to-tail transcript.

Preliminary attempts to compare the structures in solution of the *mc* ASBVd (+) and (−) RNAs by non-denaturing PAGE in 5 % gels failed to disclose a well-defined difference between their corresponding mobilities (data not shown). Although the *ml* (+) and (−) RNAs of eggplant latent viroid (ELVd, 333 nt) [35] are clearly discriminated by electrophoresis in gels of this porosity [36], they might not have sufficient power to resolve RNAs of smaller size like those of ASBVd. Therefore, we performed our experiments in 8 % gels in which, according to earlier data, *ml* ASBVd (+) and (−) RNAs migrate differentially [23]. Considering that the *in vitro* SHAPE analysis to be carried out subsequently entails a thermal denaturation/renaturation, we also tested whether such a treatment had any effect on the electrophoretic mobilities of *mc* ASBVd (+) and (−) RNAs with the same approach as used before with the two other viroids [26, 36]. In brief, prior to electrophoresis, two aliquots of each of the two RNAs under examination, resuspended in water, were heated at 95 °C for 2 min and either snap-cooled on ice or slowly cooled at 25 °C for 15 min, using a third pair of non-treated aliquots as the control. Three aliquots were then brought to 37 °C for 5 min in the folding buffer

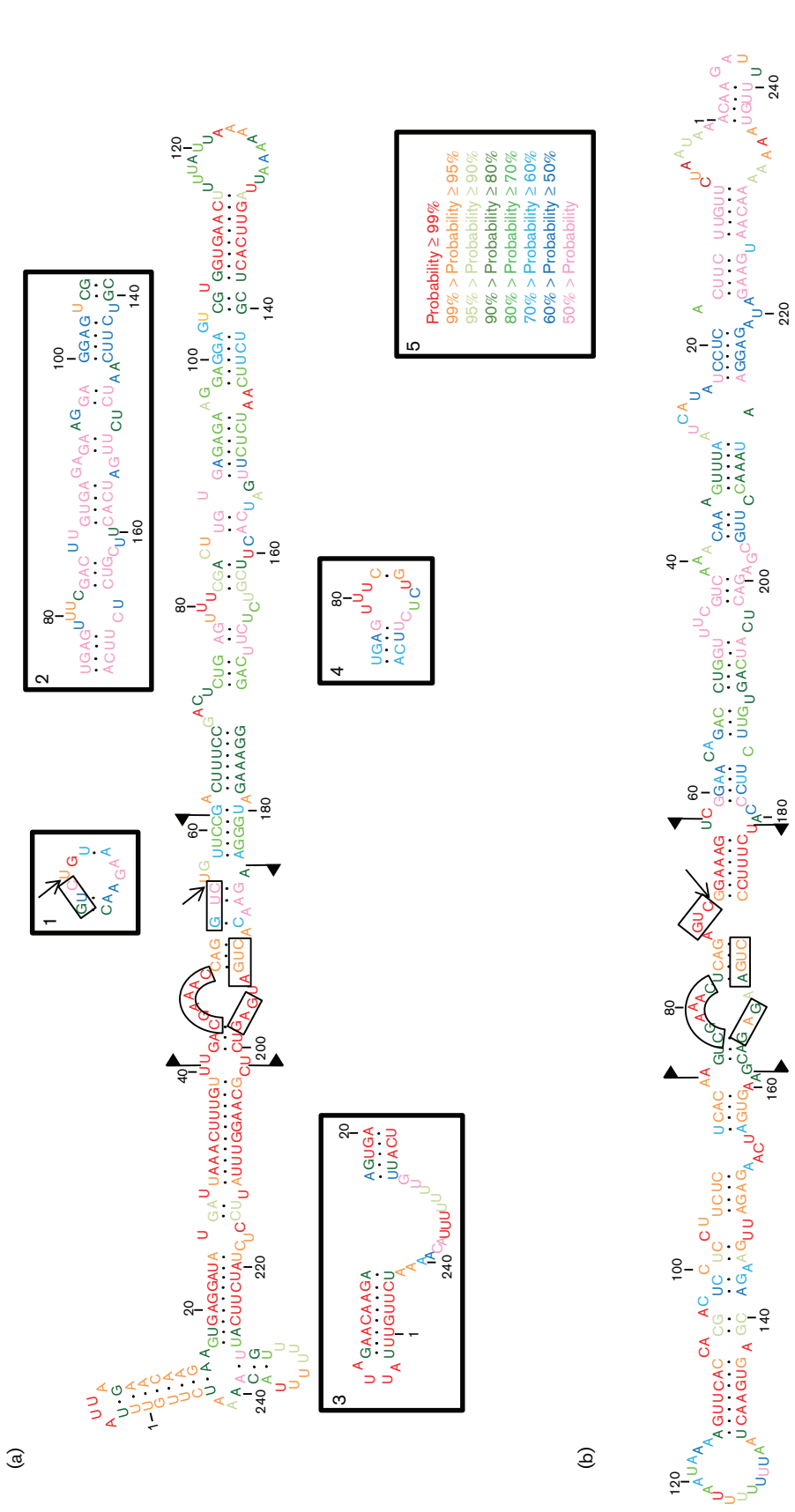

Fig. 1. Conformations of minimum free energy predicted for both strands of ASBVd (reference variant GenBank accession number J02020 with the substitution C213→U). (a) Quasi-rod-like secondary structure for the *mc* ASBVd (+) RNA predicted by *RNAstructure*. Insets (1) and (2), alternative motifs predicted by *Mfold*, and insets (1, 3) and (4), alternative motifs predicted by *RNAfold*. (b) Common rod-like secondary structure for the *mc* ASBVd (−) RNA predicted by *RNAstructure*, *RNAfold* and *Mfold*. In both panels, the sequences forming the core of the hammerhead structures are delimited by flags, motifs conserved in natural hammerhead structures are within boxes, and self-cleavage sites are marked by arrows. The same numbers are used for both polarities. Colors in inset (5) denote the probability of nucleotides being double- or single-stranded as predicted by *RNAstructure*. The conformations serving as references are those generated by *RNAstructure* because this is the software program implemented in SHAPE.

[37], with the three others being similarly treated but with the folding buffer supplemented with 6 mM Mg^{2+}. In all instances the *mc* ASBVd (+) and (−) RNAs migrated as sharp bands, supporting their adoption of a predominant conformation *in vitro* (Fig. 2a), without dismissing the co-existence of others with minor changes undetectable by non-denaturing PAGE. The lack of noticeable Mg^{2+} effects did not favour the presence of tertiary interactions like the kissing loops reported in peach latent mosaic viroid (PLMVd) and chrysanthemum chlorotic mottle viroid (CChMVd) [38, 39].

Interestingly, compared with the size markers, the *mc* ASBVd (+) RNA migrated faster than its complementary *mc* (−) form, suggesting a more compact secondary structure for the former (Fig. 2a), a result that was confirmed by co-electrophoresis of mixed aliquots of the two RNAs (Fig. 2b). As indicated above, such an observation is consistent with others made previously in gels of similar porosity, but using *ml* ASBVd (+) and (−) RNAs [23], and with the more stable conformation predicted for the *mc* ASBVd (+) RNA by the three software programs (see above). However, we found that while the *ml* ASBVd (−) RNA resulting from self-cleavage migrated in 8 % gels as a sharp band, the *ml* ASBVd (+) RNA also from self-cleavage migrated as a blurred band (data not shown), thus hinting at the co-existence of different conformations in the latter. In contrast, the *mc* ASBVd (+) form adopted a predominant conformation as inferred from its defined electrophoretic mobility (Fig. 2). This observation shows that the circular structure provides enhanced stability, at least to the (+) strand, and reinforces the advantage of performing the analyses with the *mc* ASBVd (+) and (−) RNAs rather than with their *ml* counterparts, which may not display a similar behaviour.

In vitro SHAPE with N-methylisatoic anhydride (NMIA) and 2-methylnicotinic acid imidazolide (NAI) corroborates the rod-like conformations predicted for the *mc* ASBVd (+) and (−) RNAs *in silico*

Migration of the *mc* ASBVd (+) and (−) RNAs as essentially single bands in non-denaturing PAGE was consistent with the existence in solution of predominant conformers for both polarity strands. To provide additional support for this idea at single-nucleotide resolution, we applied SHAPE *in vitro* with NMIA [37] to the *mc* ASBVd RNAs purified from infected tissue by denaturing PAGE. We first used two individual primers in order to dissect the entire *mc* ASBVd (+) RNA, with the information gained serving to generate computer-assisted predictions with *RNAstructure* [33]. Both primers produced mutually consistent data leading to a rod-shaped conformation very similar to that predicted *in silico* with *RNAfold* (Fig. 1a), thus containing a large internal asymmetric loop in the left terminal domain instead of the short bifurcation predicted by *RNAstructure* and *Mfold* (Fig. 3a). Importantly, essentially the same conformation was obtained when NMIA was replaced by NAI, the alternative acylating reagent used for *in vivo* SHAPE [26, 40, 41] (Fig. 3b).

Subsequent application of *in vitro* SHAPE to the *mc* ASBVd (−) form, again with two separate primers to examine the whole RNA, resulted in basically the same rod-like secondary structure with NMIA and NAI (Fig. 4a, b), which additionally also coincided with that predicted by the three software programs *in silico* (Fig. 1b). On the other hand, the SHAPE reactivity of some nucleotides forming the lower strand of the left terminal loop (positions 123–128) did not support their involvement in a kissing-loop interaction with the lower strand of a right terminal loop (positions 231–236) (Fig. 4a, b), as proposed previously for a *ml* ASBVd (−) form [23].

The remarkable agreement between the *in silico* and *in vitro* approaches paved the way for addressing the next issue: whether the structure of the *mc* ASBVd (+) RNA *in planta* is also the same or different. For this aim we used NAI, which for SHAPE analyses *in vivo* is preferable to NMIA because of the higher $t_{1/2}$ hydrolysis of the former [41].

SHAPE *in planta* shows that the *mc* ASBVd (+) form accumulates as a free RNA adopting a rod-shaped secondary structure without tightly bound host proteins

As indicated above we employed a NAI-based procedure [26], derived from a previous one [41], substituting 5′ primer labeling with radioactivity by a fluorophore. Moreover, as in our recent report with PSTVd [26], following NAI infiltration and incubation of ASBVd-infected leaves, and subsequent RNA extraction and clarification, the *mc* ASBVd RNAs were purified by denaturing PAGE. This step guaranteed that the observed SHAPE signals corresponded to stops taking place during reverse transcription of the *mc* ASBVd (+) RNA; the high amount of tissue (and NAI) needed made it impractical to extend this analysis *in planta* to the *mc* ASBVd (−) RNA.

Because we assumed that a limiting factor could be the penetrability of the acylating reagent, we started our studies with expanding ASBVd-infected avocado leaves (8–10 cm in length), the cuticle of which was removed with ethylic ether before their infiltration with the NAI solution. However, the resulting signals produced by the *mc* ASBVd (+) RNA were very weak and difficult to reproduce. We next moved to flowers, which according to a previous report [42] and our own observations (data not shown), accumulate high levels of ASBVd. The SHAPE signals improved but were still unsatisfactory and, besides, this plant material was only available for a short period of time. Considering these results we returned to leaves, but of a very small size (2–3 cm in length), assuming that the NAI solution would penetrate more easily than in those of bigger size. That was indeed the case, with the SHAPE signals becoming clear and reproducible (Fig. 5). Finally, we carried out an additional control in which a preparation of *mc* PSTVd (+) RNA obtained from infected tissue was added immediately after homogenization of the ASBVd-infected tissue infiltrated with NAI. The ensuing SHAPE analysis of this external RNA control failed to reveal the

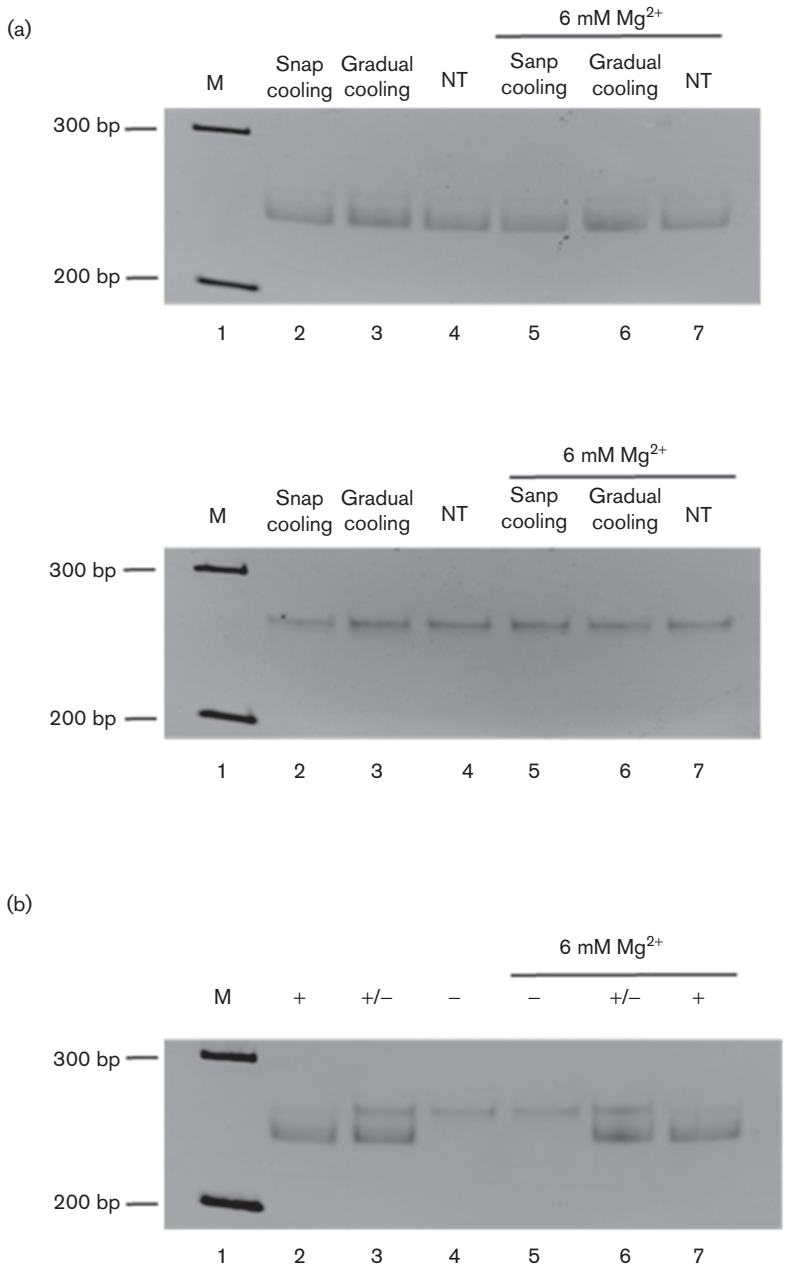

Fig. 2. *mc* ASBVd (+) and (–) RNAs show different mobilities in non-denaturing PAGE. (a) Before electrophoresis, aliquots of ASBVd (+) and (–) forms (upper and lower panels, respectively) were heated at 95 °C for 2 min and snap-cooled on ice (lane 2), gradually cooled at 25 °C for 15 min (lane 3), or applied directly with no thermal treatment (NT) (lane 4). Three other aliquots of the same RNAs were processed similarly, but in the presence of 6 mM $MgCl_2$ (lanes 5, 6 and 7, respectively). (b) Aliquots of untreated ASBVd (+) and (–) RNAs were loaded separately (lanes 2 and 4, respectively) or mixed together (lane 3). Three other aliquots of the same RNAs were processed similarly, but in the presence of 6 mM $MgCl_2$ (lanes 5, 6 and 7, respectively). M refers to DNA markers with their size (in base pairs) indicated on the left (lane 1). Gels were stained with ethidium bromide and are shown in the inverted option to facilitate visualization.

reactivity observed previously *in vitro* [26] (data not shown), thus corroborating that acylation of the *mc* ASBVd (+) RNA occurred *in planta* and not *in vitro* during the subsequent manipulations.

Comparative analyses of the *in vitro* and *in vivo* data with NAI revealed that they were essentially identical, thus supporting the notion that the *mc* ASBVd (+) RNA behaves in its physiological habitat as a free RNA folding into a rod-

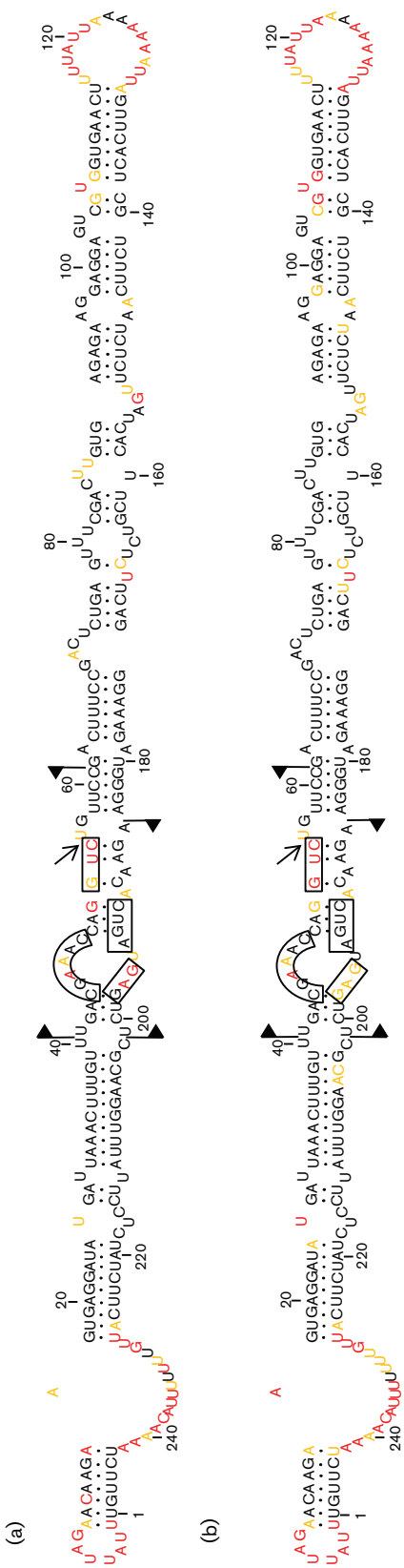

Fig. 3. *In vitro* SHAPE with NMIA (a) and NAI (b) leads to essentially the same rod-like secondary structure for the *mc* ASBVd (+) RNA. This conformation is very similar to that predicted *in silico* with *RNAfold* and contains a large internal asymmetric loop in the left terminal domain. Nucleotides in red, yellow and black displayed high (more than 0.85), intermediate (0.85–0.40) and low (less than 0.40) SHAPE-reactivity. Other details as in the legend to Fig. 1.

shaped conformation unprotected by tightly bound host proteins. In this conformation, wherein loops were generally more reactive than their flanking double-stranded helices, only two minor differences were detected: (i) the upper strand of the asymmetric loop of the left terminal domain is formed by one single (A16) and by two nucleotides (A16 and G17) in the *in vitro* and *in vivo* structures, respectively, and (ii) a small region delimited by C85 and A91 in the upper strand, and U152 and U160 in the lower strand, was slightly reorganized (Fig. 5).

DISCUSSION

For reasons explained elsewhere [2, 26, 36], viroid RNA conformations predicted *in silico* with algorithms minimizing the free-energy content, or determined *in vitro* with different biochemical and biophysical approaches, may not recapitulate the conformation existing *in vivo,* primarily because these approaches neglect the effect that RNA-binding host proteins may have on the conformation of a viroid RNA in its physiological context. In addition, RNA secondary structure is constrained by transcription, steric crowding and interacting ions [43]. Indeed, recent data indicate that the secondary structure of the *mc* (+) strand of a nuclear viroid (PSTVd) obtained by *in vivo* SHAPE, even if similar, is not identical to that observed by *in vitro* SHAPE, with the differences having been attributed to interactions with host proteins or to other factors present in the *in vivo* habitat [26].

Once the global conformation *in vivo* of the *mc* (+) form of PSTVd, the type member of the family *Pospiviroidae*, was resolved [26], application of the same methodology to a member of the family *Avsunviroidae* appeared to be the natural next step in order to test whether a general behaviour exists. Considering that conventional SHAPE *in vivo* demands relatively high viroid titres in infected tissues, we discarded PLMVd [44] and CChMVd [45] due to their poor accumulation *in planta.* Between the remaining two members of *Avsunviroidae,* the eggplant latent viroid (ELVd) [35] and ASBVd [11], we chose the latter because despite its natural host being a woody plant, the isolate of this viroid, which we have been working with over the years (GenBank accession number J02020 with the substitution C213→U), accumulates *in vivo* to levels comparable to the 5S ribosomal RNA [12, 21], much higher than those reached by ELVd in eggplant. There are modifications more sensitive than conventional SHAPE [40, 46], but some entail additional steps, particularly single-stranded adapter ligation, which limit the reliability of the results. These approaches, however, particularly SHAPE-MaP [46], may become indispensable with viroids reaching low titres *in vivo.*

Reassessment of the most stable secondary structure predicted for the *mc* ASBVd (+) RNA by three software programs resulted in a similar rod-like conformation with minor deviations. This conformation, however, differed significantly in the distribution and size of some loops and

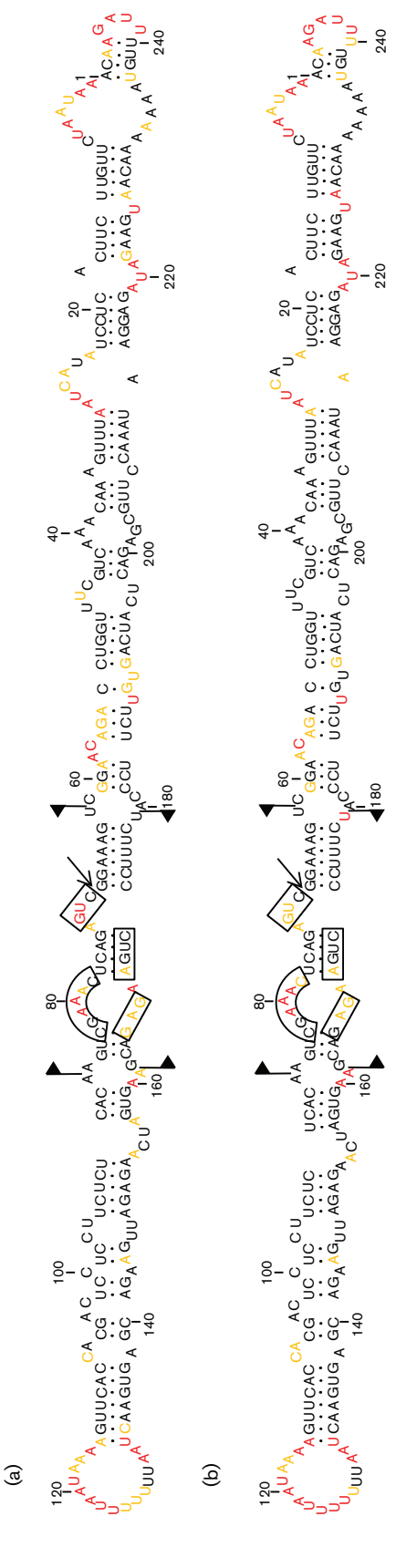

Fig. 4. *In vitro* SHAPE with NMIA (a) and NAI (b) predicts the same rod-like secondary structure for the *mc* ASBVd (−) RNA. This conformation additionally coincides with that predicted by the three software programs *in silico*. Other details as in the legends to Figs 1 and 3.

double-stranded segments when compared with others reported previously [11, 17, 20, 21]. For the *mc* ASBVd (−) RNA the agreement was even better, with the three software programs predicting the same rod-shaped secondary structure. *In vitro* SHAPE of *mc* ASBVd (+) and (−) RNAs generated well-resolved structures that were almost identical with the two acylating reagents used (NMIA and NAI), in line with the adoption of predominant conformations by both RNAs *in vitro* as inferred from their migration as single bands in non-denaturing PAGE. These structures also agree with: (i) those predicted *in silico,* particularly with the *RNAfold* software program, and (ii) those derived previously from *in vitro* SHAPE [24], while differing somewhat from others obtained with the same *in vitro* approach [23]. Furthermore, the rod-like conformations proposed *in vitro* for the *mc* ASBVd (+) and (−) RNAs are also consistent with the solubility in 2 M LiCl of the *mc* ASBVd RNAs extracted from infected tissue, mainly formed by the (+) strand [45], and of the *ml* ELVd (+) and (−) RNAs resulting from *in vitro* self-cleavage that adopt quasi-rod-like secondary structures [36]. Conversely, PLMVd and CChMVd RNAs, which fold into complex multi-branched conformations stabilized by a kissing-loop interaction, are insoluble under the same saline conditions [45]. In this same context, our *in vitro* SHAPE results do not support the existence in the *mc* ASBVd (-) RNA of the kissing-loop interaction proposed to stabilize a *ml* ASBVd (−) form, which has neither been inferred by *in vitro* SHAPE for another *ml* ASBVd (−) form [23, 24]. Moreover, we have not detected by native PAGE any Mg^{2+}-induced difference in the mobility of the *mc* ASBVd (−) RNA, while we have observed for it a slower mobility than for its (+) counterpart that neither is influenced by Mg^{2+}. This latter result, particularly, argues against the existence of a kissing-loop interaction in the *mc* ASBVd (−) RNA because an interaction of this kind in CChMVd causes a faster mobility consistent with a more compact folding [39], in contrast with the results observed in the co-electrophoresis of the *mc* ASBVd (+) and (−) RNAs (Fig. 2b).

After some preliminary assays, we found that flowers, and particularly very small expanding leaves, were the most appropriate material for *in vivo* SHAPE, probably because they are easily penetrated by NAI. Moreover, this reagent has been previously applied to determine the structure *in planta* of a chloroplast mRNA of *Arabidopsis thaliana* [40], thus indicating that NAI can traverse the membrane of this organelle. *In vivo* SHAPE of the *mc* ASBVd (+) form showed that it accumulates in chloroplasts as a free RNA uncovered by tightly bound host protein(s) which, like viral coat proteins, might exert a protecting role. However, as indicated before [26], the existence of loose or transient RNA-protein interactions, or of proteins interacting with double-stranded RNA motifs – in principle undetectable by SHAPE – cannot be dismissed, leaving to one side that chemical approaches like SHAPE infer base pairing indirectly from the absence of reactivity [43]. Pertinent to this context is the previous finding that UV irradiation of

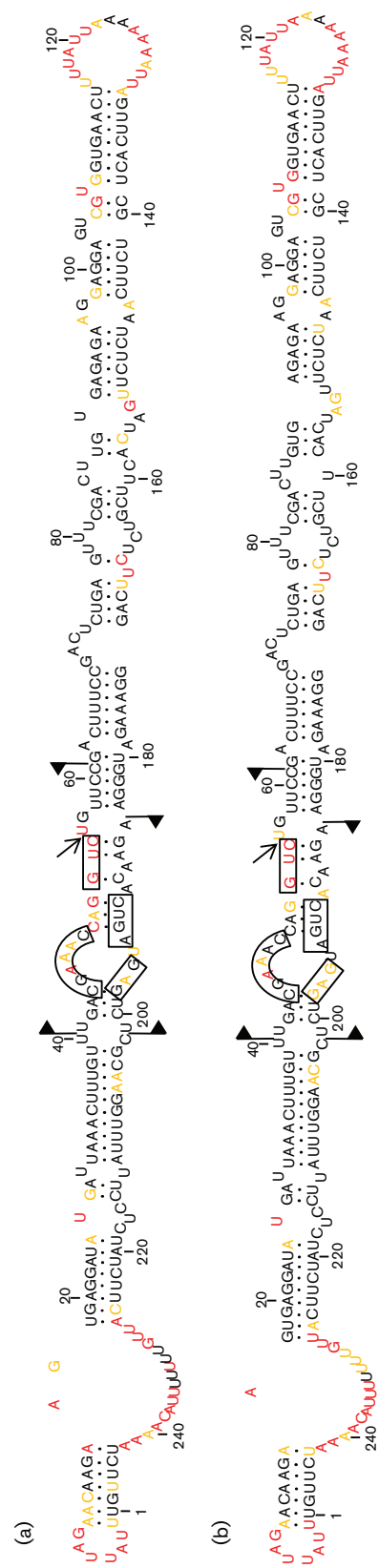

Fig. 5. *In vivo* SHAPE confirms a rod-like conformation for the *mc* ASBVd (+) RNA. (a) Results obtained with NAI *in vivo* coupled to computer-assisted prediction using *RNAstructure*. (b) Results obtained with the same acylating agent *in vitro* (see Fig. 3b) are included here to facilitate a direct comparison. Other details as in the legends to Figs 1 and 3.

ASBVd-infected avocado leaves generates covalent adducts between the *mc* ASBVd (+) RNAs and host proteins, the most abundant of which, as revealed by tandem-mass spectrometry, are two chloroplast RNA-binding proteins (PARBP33 and PARBP35) of a family involved in stabilization, maturation and editing of chloroplast transcripts. Moreover, PARBP33 behaves as an RNA chaperone that facilitates *in vitro,* and possibly *in vivo,* the self-cleavage of the oligomeric ASBVd intermediates resulting from rolling-circle replication [47]. UV light is a 'zero-length' cross-linking agent that promotes formation of covalent bonds between nucleic acids and proteins at their contact points, thus freezing the interaction existing *in situ* even if transient [48, 49]. Such cross-links, which demand close proximity and proper orientation between the reacting groups, may go unnoticed for *in vivo* SHAPE, highlighting the limitations of this latter approach and the need to combine physical and chemical strategies for proper dissection of host proteins interacting with viroid RNAs. In this regard, interactions of *mc* ASBVd RNAs with the host enzymes catalyzing replication may also be transient.

In summary, like the *mc* PSTVd (+) RNA [26], the *mc* ASBVd (+) RNA exists *in vivo* as free or 'naked' RNA that folds into a rod-like conformation without strong association with host proteins. This finding attests to the common solution evolved by two different viroids that replicate and accumulate in two different subcellular compartments, the nucleus and chloroplast. The intrinsic stability resulting from circularity and compact secondary structures promoted by double-stranded segments confer to these RNAs, and possibly to viroids in general, resistance to exonucleases and endonucleases, while some loops would play major functional roles as illustrated by the terminal A+U rich loops wherein the initiation sites of the ASBVd (+) and (−) strands have been mapped [21]. Relevant also to this framework is that there are more RNA sequences that fold into a circular than into a linear structure of the same length, implying the higher mutational robustness (i.e. resistance to mutation) of circular structures [50].

METHODS

Extraction, clarification and examination of the *mc* ASBVd RNAs

These steps were performed as reported recently [26]. In brief, total nucleic acid preparations from asymptomatic leaves from ASBVd-infected avocado plants (*Persea americana* Miller, cv. Fuerte) grown in a greenhouse (25–18 °C with supplementary lighting during the winter), were obtained with water-saturated phenol and subsequently clarified using non-ionic cellulose and methoxyethanol. The *mc* ASBVd (+) and (−) RNAs were purified by double PAGE first in a non-denaturing 5 % gel (acrylamide:bis-acrylamide ratio 39 : 1) run in 1X TAE at 4 °C, with the segment demarcated by the DNA markers of 200 and 300 bp being excised and applied on top of a single-well 5 % denaturing gel of the same porosity that was run in 0.25X TBE

(final gel temperature around 50 °C). The band of interest was cut and its RNAs gel-eluted overnight and examined by non-denaturing PAGE in 5 or 8 % gels, the latter with an acrylamide:bis-acrylamide ratio 19 : 1, run in 1X TAE at 4 °C. The *mc* ASBVd (−) RNA was prepared by incubation at 25 °C for 2 h of gel-purified *ml* ASBVd (−) RNA (5 µg), resulting from *in vitro* self-cleavage of a dimeric head-to-tail transcript, in a final volume of 50 µl containing 25 µl of a wheat germ extract (Promega) and 40 U of the ribonuclease inhibitor from porcine liver (Takara).

Prediction of RNA structure *in silico*

Three software programs were applied to retrieve the structures of minimal free energy of the *mc* ASBVd (+) and (−) RNAs: *Mfold* version 4.7 [30] and *RNAfold* included in the ViennaRNA package version 2.3.1 [32] using the circular versions and default parameters, and *RNAstructure* version 5.8 (Shapeknots) [33, 34] using the default parameters and beginning the numbering from the self-cleavage sites.

In vitro SHAPE

The mixture of *mc* ASBVd (+) and (−) RNAs purified from infected avocado leaves were subjected to *in vitro* SHAPE with N-methylisatoic anhydride (NMIA, 13 mM in dimethyl-sulfoxide) essentially as described previously [26, 37]; when analysing the (+) and (−) forms, 3 and 30 pmol of the RNA mixture were used, respectively. SHAPE *in vitro* with 2-methylnicotinic acid imidazolide (NAI, 50 mM in dimethyl-sulfoxide) was carried out similarly, being NAI prepared as reported before [41]. The resulting data were coupled to computer-assisted prediction [33]. VIC-labelled fluorescent DNA primers (Applied Biosystems) RF-1370 (5′-CAGACCTGGTTTCGTC-3′) and RF-1378 (5′-CCC TGAAAGGACGAAGTGATCAAGAG-3′), complementary to positions 57–42 and 174–149, respectively, and RF-1387 (5′-CTCTGAGTTTCGACTTGTGAGAGAAGG-3′) and RF-1388 (5′-GATGGGAAGAACACTGATGAGTCTCGC-3′) homologous to positions 72–98 and 178–204 respectively, were purified by denaturing PAGE in 20 % gels. Extensions, sequencing reactions to identify the peaks, and resolution of the cDNAs by capillary electrophoresis were as detailed previously [26, 51]. Electrophoregrams were examined with the QuShape software program [52], which also normalized the reactivity data. At least three replicas were analysed with each primer and acylating reagent, and the mean and standard deviation of the reactivity of each nucleotide was calculated.

In vivo SHAPE

Young leaves (3 g) of different size (see Results) of ASBVd-infected avocado, pre-treated with ethylic ether to remove the cuticle, were mixed with 50 ml of buffer (40 mM HEPES-NaOH pH 7.5, 100 mM KCl, 0.5 mM $MgCl_2$) and gently shaken for 5 min. *In planta* acylation was performed by incorporating NAI (100 mM in dimethylsulfoxide and just dimethylsulfoxide to the control reaction) and shaking the mixture at room temperature for 40 min. Following addition of β-mercaptoethanol (500 mM) and shaking for another 10 min to stop the reaction, the leaves were drained and washed four times with water (100 ml). Extraction, clarification, purification and primer-extension of the *mc* ASBVd (+) RNA was the same as with *in vitro* SHAPE. Six replicas were performed with each primer, and the mean and standard deviation of the reactivity of each nucleotide were estimated.

Funding information
This work was supported by grant BFU2014-56812-P (to R. F.) from the Ministerio de Economía y Competitividad of Spain. A. L. C. was the recipient of a predoctoral fellowship from the same organization.

Acknowledgements
We thank Drs Cristina Romero and Alicia Barroso for their valuable help with the initial SHAPE experiments, Drs Sonia Delgado and Pedro Serra for helpful advise, and A. Ahuir and M. Pedrote for excellent technical assistance.

Conflicts of interest
The authors declare that there are no conflicts of interest.

References

1. Diener TO. Discovering viroids–a personal perspective. *Nat Rev Microbiol* 2003;1:75–80.
2. Flores R, Serra P, Minoia S, di Serio F, Navarro B. Viroids: from genotype to phenotype just relying on RNA sequence and structural motifs. *Front Microbiol* 2012;3:217.
3. Flores R, Minoia S, Carbonell A, Gisel A, Delgado S *et al.* Viroids, the simplest RNA replicons: how they manipulate their hosts for being propagated and how their hosts react for containing the infection. *Virus Res* 2015;209:136–145.
4. Katsarou K, Rao AL, Tsagris M, Kalantidis K. Infectious long non-coding RNAs. *Biochimie* 2015;117:37–47.
5. Kovalskaya N, Hammond RW. Molecular biology of viroid-host interactions and disease control strategies. *Plant Sci* 2014;228:48–60.
6. Palukaitis P. What has been happening with viroids? *Virus Genes* 2014;49:175–184.
7. Steger G, Perreault JP. Structure and associated biological functions of viroids. *Adv Virus Res* 2016;94:141–172.
8. Palukaitis P, Hatta T, Alexander DM, Symons RH. Characterization of a viroid associated with avocado sunblotch disease. *Virology* 1979;99:145–151.
9. Flores R, Hernández C, Martínez de Alba AE, Daròs JA, di Serio F. Viroids and viroid-host interactions. *Annu Rev Phytopathol* 2005;43:117–139.
10. Owens RA, Flores R, Di Serio F, Li F, Pallás V *et al.* Virus taxonomy. In: King AMQ, Adams MJ, Carstens EB and Lefkowitz EJ (editors). *Ninth Report of the International Committee on Taxonomy of Viruses*. London, UK: Elsevier/Academic Press; 2012. pp. 1221–1234.
11. Symons RH. Avocado sunblotch viroid: primary sequence and proposed secondary structure. *Nucleic Acids Res* 1981;9:6527–6537.
12. Bruening G, Gould AR, Murphy PJ, Symons RH. Oligomers of avocado sunblotch viroid are found in infected avocado leaves. *FEBS Lett* 1982;148:71–78.
13. Daròs JA, Marcos JF, Hernández C, Flores R. Replication of avocado sunblotch viroid: evidence for a symmetric pathway with two rolling circles and hammerhead ribozyme processing. *Proc Natl Acad Sci USA* 1994;91:12813–12817.
14. Hutchins CJ, Keese P, Visvader JE, Rathjen PD, Mcinnes JL *et al.* Comparison of multimeric plus and minus forms of viroids and virusoids. *Plant Mol Biol* 1985;4:293–304.

15. Navarro JA, Darós JA, Flores R. Complexes containing both polarity strands of avocado sunblotch viroid: identification in chloroplasts and characterization. *Virology* 1999;253:77–85.
16. Navarro JA, Vera A, Flores R. A chloroplastic RNA polymerase resistant to tagetitoxin is involved in replication of avocado sunblotch viroid. *Virology* 2000;268:218–225.
17. Hutchins CJ, Rathjen PD, Forster AC, Symons RH. Self-cleavage of plus and minus RNA transcripts of avocado sunblotch viroid. *Nucleic Acids Res* 1986;14:3627–3640.
18. Carbonell A, de la Peña M, Flores R, Gago S. Effects of the trinucleotide preceding the self-cleavage site on eggplant latent viroid hammerheads: differences in co- and post-transcriptional self-cleavage may explain the lack of trinucleotide AUC in most natural hammerheads. *Nucleic Acids Res* 2006;34:5613–5622.
19. Nohales MÁ, Molina-Serrano D, Flores R, Daròs JA. Involvement of the chloroplastic isoform of tRNA ligase in the replication of viroids belonging to the family *Avsunviroidae*. *J Virol* 2012;86:8269–8276.
20. Gast FU, Kempe D, Spieker RL, Sänger HL. Secondary structure probing of potato spindle tuber viroid (PSTVd) and sequence comparison with other small pathogenic RNA replicons provides evidence for central non-canonical base-pairs, large A-rich loops, and a terminal branch. *J Mol Biol* 1996;262:652–670.
21. Navarro JA, Flores R. Characterization of the initiation sites of both polarity strands of a viroid RNA reveals a motif conserved in sequence and structure. *Embo J* 2000;19:2662–2670.
22. Steger G, Hofmann H, Förtsch J, Gross HJ, Randles JW *et al.* Conformational transitions in viroids and virusoids: comparison of results from energy minimization algorithm and from experimental data. *J Biomol Struct Dyn* 1984;2:543–571.
23. Delan-Forino C, Deforges J, Benard L, Sargueil B, Maurel MC *et al.* Structural analyses of avocado sunblotch viroid reveal differences in the folding of plus and minus RNA strands. *Viruses* 2014;6:489–506.
24. Giguère T, Adkar-Purushothama CR, Bolduc F, Perreault JP. Elucidation of the structures of all members of the *Avsunviroidae* family. *Mol Plant Pathol* 2014;15:767–779.
25. Hui-Bon-Hoa G, Kaddour H, Vergne J, Kruglik SG, Maurel MC. Raman characterization of avocado sunblotch viroid and its response to external perturbations and self-cleavage. *BMC Biophys* 2014;7:2.
26. López-Carrasco A, Flores R. Dissecting the secondary structure of the circular RNA of a nuclear viroid *in vivo:* a "naked" rod-like conformation similar but not identical to that observed *in vitro*. *RNA Biol* 2017, doi: 10.1080/15476286.2016.1223005.
27. Bonfiglioli RG, Mcfadden GI, Symons RH. *In situ* hybridization localizes avocado sunblotch viroid on chloroplast thylakoid membranes and coconut cadang cadang viroid in the nucleus. *Plant J* 1994;6:99–103.
28. Lima MI, Fonseca ME, Flores R, Kitajima EW. Detection of avocado sunblotch viroid in chloroplasts of avocado leaves by in situ hybridization. *Arch Virol* 1994;138:385–390.
29. Mohamed NA, Thomas W. Viroid-like properties of an RNA species associated with the sunblotch disease of avocados. *J Gen Virol* 1980;46:157–167.
30. Zuker M. Mfold web server for nucleic acid folding and hybridization prediction. *Nucleic Acids Res* 2003;31:3406–3415.
31. Riesner D, Steger G. Viroid and viroid-like RNA. In: Saenger W (editor). *Landolt-Börnstein, New Series in Biophysics – Nucleic Acids*. Berlin: Springer-Verlag; 1990. vol. VII, pp. 194–243.
32. Lorenz R, Bernhart SH, Höner Zu Siederdissen C, Tafer H, Flamm C *et al.* ViennaRNA package 2.0. *Algorithms Mol Biol* 2011;6:26.
33. Hajdin CE, Bellaousov S, Huggins W, Leonard CW, Mathews DH *et al.* Accurate SHAPE-directed RNA secondary structure modeling, including pseudoknots. *Proc Natl Acad Sci USA* 2013;110:5498–5503.
34. Reuter JS, Mathews DH. RNAstructure: software for RNA secondary structure prediction and analysis. *BMC Bioinformatics* 2010;11:129.
35. Fadda Z, Daròs JA, Fagoaga C, Flores R, Duran-Vila N. Eggplant latent viroid, the candidate type species for a new genus within the family *Avsunviroidae* (hammerhead viroids). *J Virol* 2003;77:6528–6532.
36. López-Carrasco A, Gago-Zachert S, Mileti G, Minoia S, Flores R *et al.* The transcription initiation sites of eggplant latent viroid strands map within distinct motifs in their *in vivo* RNA conformations. *RNA Biol* 2016;13:83–97.
37. Wilkinson KA, Merino EJ, Weeks KM. Selective 2'-hydroxyl acylation analyzed by primer extension (SHAPE): quantitative RNA structure analysis at single nucleotide resolution. *Nat Protoc* 2006;1:1610–1616.
38. Bussière F, Ouellet J, Côté F, Lévesque D, Perreault JP. Mapping in solution shows the peach latent mosaic viroid to possess a new pseudoknot in a complex, branched secondary structure. *J Virol* 2000;74:2647–2654.
39. Gago S, de la Peña M, Flores R. A kissing-loop interaction in a hammerhead viroid RNA critical for its *in vitro* folding and *in vivo* viability. *RNA* 2005;11:1073–1083.
40. Kwok CK, Ding Y, Tang Y, Assmann SM, Bevilacqua PC. Determination of *in vivo* RNA structure in low-abundance transcripts. *Nat Commun* 2013;4:2971.
41. Spitale RC, Crisalli P, Flynn RA, Torre EA, Kool ET *et al.* RNA SHAPE analysis in living cells. *Nat Chem Biol* 2013;9:18–20.
42. da Graça JV, Mason TE. Detection of avocado sunblotch viroid in flower buds by *Polyacrylamide* gel electrophoresis. *J Phytopathology* 1983;108:262–266.
43. Vandivier LE, Anderson SJ, Foley SW, Gregory BD. The conservation and function of RNA secondary structure in plants. *Annu Rev Plant Biol* 2016;67:463–488.
44. Hernández C, Flores R. Plus and minus RNAs of peach latent mosaic viroid self-cleave *in vitro* via hammerhead structures. *Proc Natl Acad Sci USA* 1992;89:3711–3715.
45. Navarro B, Flores R. Chrysanthemum chlorotic mottle viroid: unusual structural properties of a subgroup of self-cleaving viroids with hammerhead ribozymes. *Proc Natl Acad Sci USA* 1997;94:11262–11267.
46. Smola MJ, Rice GM, Busan S, Siegfried NA, Weeks KM. Selective 2'-hydroxyl acylation analyzed by primer extension and mutational profiling (SHAPE-MaP) for direct, versatile and accurate RNA structure analysis. *Nat Protoc* 2015;10:1643–1669.
47. Daròs JA, Flores R. A chloroplast protein binds a viroid RNA *in vivo* and facilitates its hammerhead-mediated self-cleavage. *Embo J* 2002;21:749–759.
48. Hockensmith JW, Kubasek WL, Vorachek WR, Evertsz EM, von Hippel PH. Laser cross-linking of protein-nucleic acid complexes. *Methods Enzymol* 1991;208:211–236.
49. Pashev IG, Dimitrov SI, Angelov D. Crosslinking proteins to nucleic acids by ultraviolet laser irradiation. *Trends Biochem Sci* 1991;16:323–326.
50. Cuesta JA, Manrubia S. Enumerating secondary structures and structural moieties for circular RNAs. *J Theor Biol* 2017;419:375–382.
51. Mortimer SA, Weeks KM. Time-resolved RNA SHAPE chemistry: quantitative RNA structure analysis in one-second snapshots and at single-nucleotide resolution. *Nat Protoc* 2009;4:1413–1421.
52. Karabiber F, Mcginnis JL, Favorov OV, Weeks KM. QuShape: rapid, accurate, and best-practices quantification of nucleic acid probing information, resolved by capillary electrophoresis. *RNA* 2013;19:63–73.